INFLUENCE OF WELD-PROCESS PARAMETERS ON THE MATERIAL CHARACTERIZATION OF THE FRICTION-STIR-WELDED JOINTS OF THE AA6061-T$_6$ ALUMINIUM ALLOY

VPLIV PARAMETROV POSTOPKA VARJENJA NA LASTNOSTI TORNO-VRTILNO VARJENIH SPOJEV ALUMINIJEVE ZLITINE AA6061-T$_6$

Hiralal Patil[1], Sanjay Soman[2]

[1]Department of Mechanical Engineering, GIDC Degree Engineering College, Abrama-Navsari, India
[2]Department of Metallurgy & Material Engineering, Faculty of Engineering & Technology, M. S. University of Baroda, India
hspatil12@rediffmail.com, hspatil28@gmail.com

Friction-stir welding (FSW), a solid-state innovative joining technique, is being widely used for joining aluminium alloys for the aerospace, marine, automotive industries and many other applications of commercial importance. FSW trials were carried out using a vertical machining centre (VMC) on an AA6061 alloy. The main objective of the present work was to evaluate the weld-processing parameters of FSW for the AA6061-T$_6$ alloy and to determine the properties of the obtained joints with respect to the welding speed. The experiments were conducted by varying the welding speed between 55–70 mm/min and the rotating speed was fixed at 1700 r/min. The tensile properties, microstructure, microhardness, fractography and corrosion resistance of the FSW joints were investigated in this study. The result showed that there was a variation in the grain size in each weld zone depending upon the material and the process parameters of FSW in a joint. The coarsest grain size was observed in the heat-affected zone (HAZ), followed by the thermo-mechanically affected zone (TMAZ) and the nugget zone (NZ). The maximum tensile strength of 184 MPa and the highest joint efficiency of 49.32 % were obtained on the joint fabricated at the welding speed of 55 mm/min.

Keywords: friction-stir welding, AA6061 aluminium alloy, mechanical and metallurgical characterization, corrosion

Torno-vrtilno varjenje (FSW) je inovativna tehnika spajanja v trdnem stanju za spajanje aluminijevih zlitin za letalstvo, pomorsko, avtomobilsko industrijo in mnoge druge komercialno pomembne uporabe. FSW-preizkusi so bili izvedeni na vertikalnem obdelovalnem stroju (VMC) z zlitino AA6061. Glavni cilj tega dela je bila ocena varilnih parametrov pri FSW-postopku pri zlitini AA6061-T$_6$ in določitev lastnosti dobljenih spojev glede na hitrost varjenja. Preizkusi so bili izvršeni pri različnih hitrostih varjenja 55–70 mm/min, pri čemer je bila hitrost rotacije stalna pri 1700 r/min. V tej študiji so bile preizkušene natezna trdnost, mikrostruktura, mikrotrdota, fraktografija in korozijska odpornost FSW-spojev. Rezultati so pokazali, da se je je v vsaki coni varjenja spreminjala velikost zrn, kar je posledica materiala in procesnih parametrov pri FSW-spoju. Najbolj groba zrna se opazi v toplotno vplivani coni (HAZ), sledi ji termomehansko vplivano področje (TMAZ) in drobnozrnato področje (NZ). Največja natezna trdnost 184 MPa in največja učinkovitost spajanja 49,32 % sta bili doseženi pri spoju s hitrostjo varjenja 55 mm/min.

Ključne besede: torno-vrtilno spajanje, aluminijeva zlitina AA6061, mehansko-metalurška karakterizacija, korozija

1 INTRODUCTION

AA6061-T$_6$ alloys are high-strength aluminium (Al), magnesium (Mg) and silicon (Si) alloys containing manganese to increase their ductility and toughness. The alloys of this class are readily weldable, but they suffer from a severe softening in the heat-affected zone (HAZ) because of the dissolution of the Mg$_2$Si precipitates during the thermal cycle. It is therefore appropriate to overcome or minimize the HAZ softening with respect to the fusion welding in order to improve the mechanical properties of a weldment.[1] In addition, a poor solidification microstructure and porosity in the fusion zone should also be overcome. Compared to many of the fusion-welding processes that are routinely used for joining structural alloys, friction-stir welding (FSW) is an emerging solid-state joining process, in which the material that is being welded does not melt and recast.

FSW is a solid-state process based on plastic deformation. FSW is a continuous, hot-shear, autogenous process involving a non-consumable rotating tool of a material harder than the substrate material. Defect-free welds with good mechanical properties have been made of a variety of aluminium alloys, even those previously thought not to be weldable. When alloys are friction-stir welded, the phase transformations occurring during the cooling down of a weld are of a solid-state type. Due to the absence of the parent-metal melting, the new FSW process is found to have several advantages over the fusion welding.[2–4] In this process a special pin/slug rotating at a high speed penetrates to the centre of the two pieces to be joined. The heat generated through friction makes the material soften into a paste-like phase (plasticize).[5] Plastic deformation causes the edges of the material to mix together and fuse, hence the term "fric-
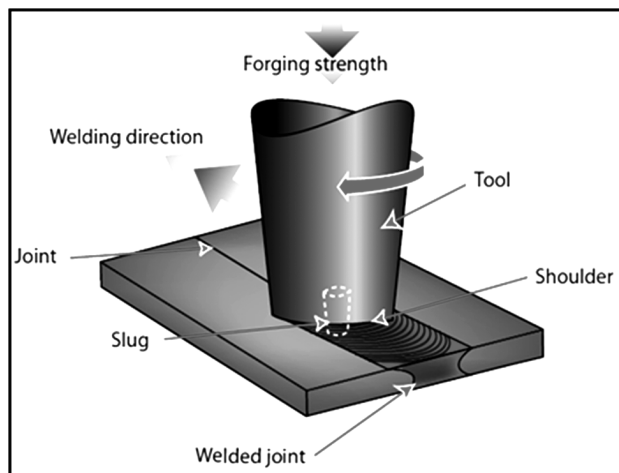
Figure 1: Principle of the FSW process
Slika 1: Princip FSW-postopka

tion-stir weld". The presence of a retaining wall exerts sufficient force to prevent the semi-molten mixture from flowing out of the joint area. This creates a press forging effect behind the material which has been softened and mixed. Welding by plastic deformation is the technique of choice when maintaining the original properties of the metal is all-important. Since the tool heats the material to a paste-like consistency, and not the liquid state, the properties of the material are not degraded to the same degree as they are when fusion occurs. **Figure 1** explains the working principle of the FSW process.

FSW has a quality advantage of making the weld strength and ductility either identical or better than those of the base-metal alloy.[6] The tensile strength of FSW welds is directly proportional to the welding speed.[7] Friction-stir processing (FSP) is a new microstructural modifications technique. FSP has become an efficient tool for homogenizing and refining the grain structure of a metal sheet. The tensile strength of the friction-stir welds is affected by the weld parameter. The grain structure within the friction-stir processing is fine and equiaxed compared to TMAZ.[8] An optimization of the FSW parameters in different conditions of a base material and the microstructures of the as-welded condition are compared with the post-weld heat-treated microstructures welded in the annealed and T_6 condition.[9] FSW joints usually consist of four different regions as shown

A - Weld Nugget, B-Thermo-Mechanically Affected zone (TMAZ) , C-Heat Affected Zone(HAZ), D-Parent material
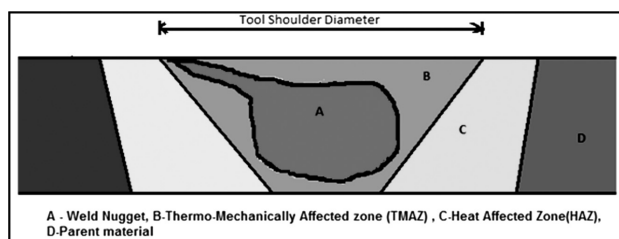
Figure 2: Different regions of a FSW joint
Slika 2: Različna področja v FSW-spoju

in **Figure 2**. They are: A-weld nugget (WN), B-thermo-mechanically affected zone (TMAZ), C-heat-affected zone (HAZ) and D-parent material (PM). The formation of the above regions is affected by the material flow behaviour under the action of rotating a non-consumable tool.[10] However, the material flow behaviour is predominantly influenced by the FSW tool profiles, FSW tool dimensions and FSW process parameters.[11,12]

The weld zones are more susceptible to corrosion than the parent metal.[13–18] Generally, it has been found that friction-stir (FS) welds of aluminium alloys such as 2219, 2195, 2024, 7075 and 6013 did not exhibit an enhanced corrosion of the weld zones. FSWs of aluminium alloys exhibit intergranular corrosion mainly located along the nugget's heat-affected zone (HAZ) enhanced by the coarsening of the grain-boundary precipitates. Coarse precipitates and wide precipitate-free zones promoted by the thermal excursion during the welding are correlated with the intergranular corrosion. The effect of the FSW parameters on the corrosion behavior of friction-stir welded joints was reported by many researchers.[16,18] The effect of the processing parameters such as the rotation speed and traverse speed on the corrosion behavior of the friction-stir processed, high-strength, precipitation-hardenable AA2219-T87 alloy was investigated by Surekha et al.[18] The available literature focuses on the effect of tool profiles and tool shoulder diameter on the FSW zone formation. Hence, in this investigation an attempt has been made to understand the effect of the welding speed on the material characterization of AA6061 in terms of mechanical properties, metallurgical behaviour and corrosion analysis. This paper presents the effects of different welding speeds on the weld characteristics of AA6061-T_6 fabricated with a hexagonal tool-pin profile. The weld characteristics include UTS, YS and a fraction of elongation, microhardness, fractography, microstructure and corrosion of AA6061-T_6 joints.

2 EXPERIMENTAL DETAILS AND PROCESS CONDITIONS

The rolled plates with a thickness of 5 mm, made of AA6061 aluminium alloy, were cut into the required shapes (300 mm × 150 mm) by power hacksaw cutting and grinding. The chemical composition and mechanical properties of the parent metal are presented in **Table 1**. A square-butt joint configuration was prepared to fabricate the FSW joints. The initial joint configuration was obtained by securing the plates in the position using mechanical clamps. The direction of welding was normal to the rolling direction. The single-pass welding procedure was adopted to fabricate the joints. In the present work a hexagonal, tool-pin profile was used for the welds, made of cold-work die steel (**Figure 3**). The machine used for the production of the joints was a vertical machining centre.

Table 1: Chemical composition and mechanical properties of AA6061-T$_6$
Tabela 1: Kemijska sestava in mehanske lastnosti AA6061-T$_6$

Chemical composition								
Element	Si	Fe	Cu	Mn	Mg	Cr	Zn	Ti
Content	0.62	0.45	0.2	0.18	1.05	0.09	0.03	0.07
Mechanical properties								
Tensile strength (MPa)		Yield strength (MPa)		Elongation (%)		Hardness (HV)		
Min	Max	Min	Max	Min	Max			
300	–	241	–	6	–	95		
328.57	335.71	282	296	11	11.8	98		
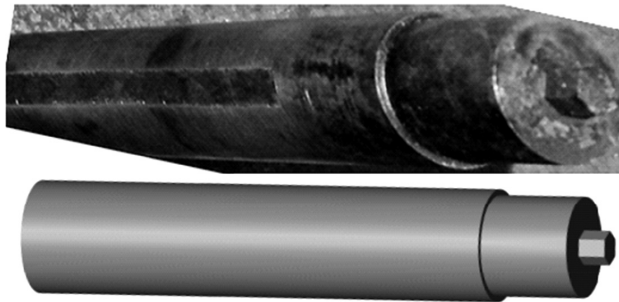
Figure 3: Geometry of the hexagonal tool-pin profile used in the present study
Slika 3: Geometrija šesterokotne konice, uporabljene pri preiskavah

The welding parameters and tool dimensions are presented in **Table 2**. The welded joints were sliced, using a pantograph machine, to the required dimensions to prepare the tensile specimens. American Society for Testing of Materials (ASTM E8-04) guidelines were followed when preparing the test specimens. The tensile test was carried out in a 400 kN capacity, mechanically controlled, universal testing machine.

Table 2: Welding conditions employed to join the AA6061 plates
Tabela 2: Pogoji varjenja, uporabljeni pri spajanju AA6061-plošč

Weld process parameter	Value
Rotational speed (r/min)	1700
Welding speed (mm/min)	55, 60, 65, 70
Tool depth (mm)	4.6
Tool shoulder diameter (mm)	18
Tilt angle (degree)	0
Hexagonal shape (mm)	6

All the welded samples were visually inspected to verify a presence of possible macroscopic external defects, such as surface irregularities, excessive flash and surface-open tunnels. By using a radiographic unit, an X-ray radiographic inspection was carried out on the FSW samples. For the radiographic test, 6Ci & Ir192 were used as a radioactive source. The film used was Agfa D-4 and the radiographic films indicated a defect-free weld as well as a weld with defects like insufficient fusion and cavity.

The mechanical properties of the test welds were assessed with the tensile tests; the ultimate tensile stress (UTS), yield strength (YS) and the fraction of elongation were also measured with the tensile test. The micro-indentation hardness test as per ASTM E-384:2006 was used to measure the Vickers hardness of the FSW joints. The Vickers micro-hardness indenter is made of diamond in the form of a square-based pyramid. The test load applied was 100 g and the dwell time was 15 s. The indentations were made in the midsections of the plates, across the joint. The tensile-fracture surfaces were analyzed using scanning electron microscopy.

The metallographic specimens were cut out mechanically from the welds, embedded in resin and mechanically ground and polished using abrasive disks and cloths with a water suspension of diamond particles. The chemical etchant was the Keller's reagent. The microstructures were observed with an optical microscope.

Potentiodynamic polarization tests were used to study the pitting corrosion behavior of AA6061 alloys. In the tests, the cell-current readings were taken during a short, slow sweep of the potential. The sweep was taken in the range of 0.5 V to 1 V. The potentiodynamic scan was performed at the scan rate of 0.5 mV/s.

3 RESULT AND DISCUSSION

3.1 Mechanical properties

The mechanical and metallurgical behavior of AA6061 was studied in this research. The transverse tensile properties of FSW joints such as yield strength, tensile strength, percentage of elongation and joint efficiency are presented in **Figure 4**. The strength and ductility in the as-welded condition are lower than in the case of the parent metal in the T$_6$ condition.

The heat input in the weld area is affected by the welding conditions like the welding speed and rotational speed. At a constant rotational speed of 1700 r/min (**Figure 5**), a higher welding speed resulted in a lower heat input per unit length of the weld, causing a lack of stirring in the friction-stir processing zone and poor tensile properties. A lower welding speed resulted in a higher temperature and a slower cooling rate in the weld zone causing grain growth and precipitates. Most of the joint fractures at the retreating side are due to the variation in the temperature distribution and the flow of the material in the weld zone with the corresponding hardness distribution and strained region. It can be observed that the flows of the parent material on the
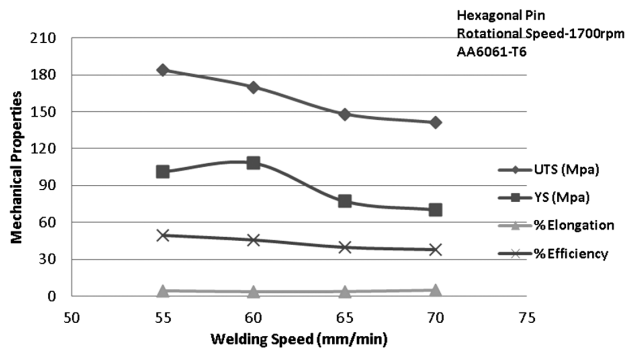
Figure 4: Effect of the welding speed on the mechanical properties of AA6061-T$_6$
Slika 4: Vpliv hitrosti varjenja na mehanske lastnosti AA6061-T$_6$

advancing side and the retreating side are different. The material on the retreating side never enters the rotational zone, but the material on the advancing side forms a fluidized bed near the pin and rotates around it (**Figure 6**). The downward (axial) force was found to be independent of the process parameter values for this experimental-data set, providing the position control. It has been observed that the axial force is a quality indicator for friction-stir welds. An insufficient axial force indicates a lack of the shoulder pressure and can also indicate a lack of the containment of the surface flash and/or voids.

During FSW the heat is assumed to be produced mainly through the friction between the tool shoulder and the plate surface. Therefore, the heat is no longer concentrated to a narrow line, but is generated across a broad band having the width of the tool shoulder. Hence, the tangential velocity of the rotating tool-shoulder surface is high at the periphery; the strongest temperature gradients are not expected to be found in the weld line but at the edges of the shoulder resulting in a thermal softening. The location of the soft band is at the retreating side, where the over-aging precipitates cause a failure in this region. Hence, the welding speed must be optimized to get an FSP region with fine precipitates uniformly distributed throughout the matrix. Of the four
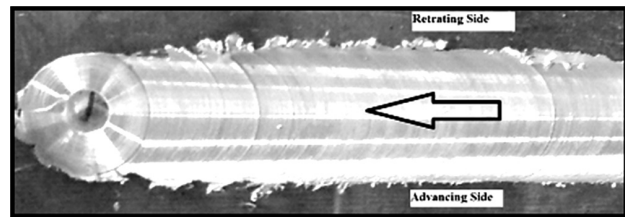
Figure 6: Friction-stir welded joint of AA6061-T$_6$
Slika 6: Torno-vrtilni varjeni spoj AA6061-T$_6$

different welding speeds (55–70 mm/min), the joints fabricated at the welding speed of 55 mm/min exhibited superior tensile properties – the ultimate tensile strength of 184 N/mm^2 and the joint efficiency of 49.32 %. The combined effect of a higher number of the pulsating, stirring actions during the metal flow and an optimum welding speed may be the reason for the superior tensile properties of the joint fabricated at a welding speed of 55 mm/min using a hexagonal, pin-profiled tool (**Figures 4 and 5**).

In FSW, microhardness also reflects the state of the precipitates within the weld nugget (WN) since the alloy composition is fixed and the changes in the microhardness must result primarily from the changes in the precipitates and the grain size. The microhardness plots for the welds of the AA6061 alloy performed with different welding speeds can be seen in **Figure 7**. The results show that the friction-stir-processed area has an equivalent Vickers hardness value with respect to the parent material.

3.2 Metallographic analysis

Based on the optical microstructural characterization of the grains and precipitates, three distinct zones were identified: the weld-nugget zone, the thermo-mechanically affected zone (TMAZ) and the heat-affected zone (HAZ). Microstructural details of the parent metals (PM) and similar joints are presented in **Figures 8** to **10**. The parent material revealed grains of unequal sizes and was found to be distributed in the matrix with the grains tending to be rather elongated. The frictional heat pro-
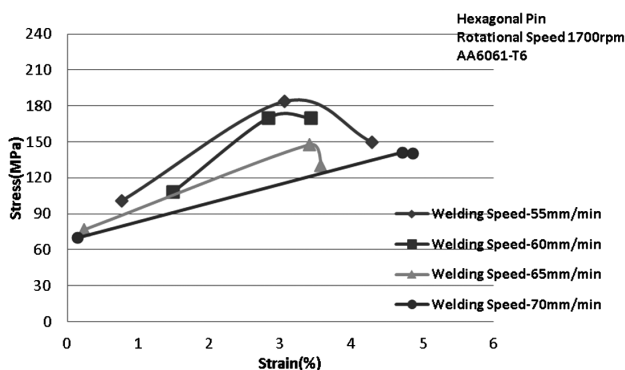
Figure 5: Engineering stress-strain curves for AA6061-T$_6$ with a hexagonal pin
Slika 5: Inženirske krivulje napetost – raztezek za AA6061-T$_6$ pri šestkotni konici
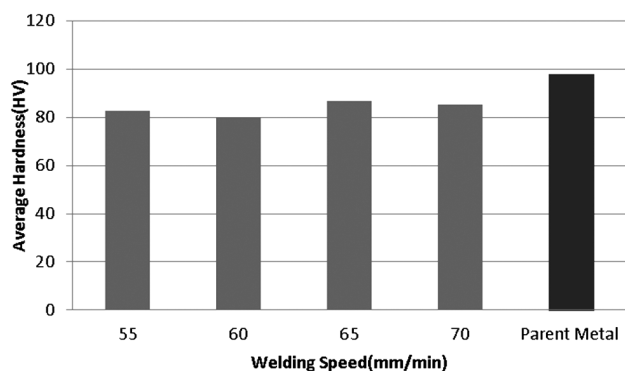
Figure 7: Effect of the welding speed on the microhardness of AA6061-T$_6$
Slika 7: Vpliv hitrosti varjenja na mikrotrdoto AA6061-T$_6$
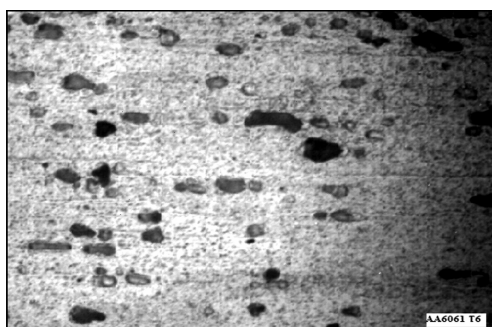
Figure 8: Optical micrograph of the AA6061 parent metal
Slika 8: Mikrostruktura osnovnega materiala AA6061
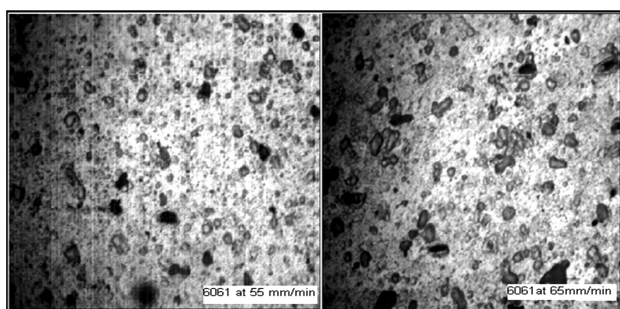
Figure 9: Optical micrograph of AA6061 at 55 mm/min and 65 mm/min
Slika 9: Mikrostruktura spoja AA6061 pri 55 mm/min in 65 mm/min
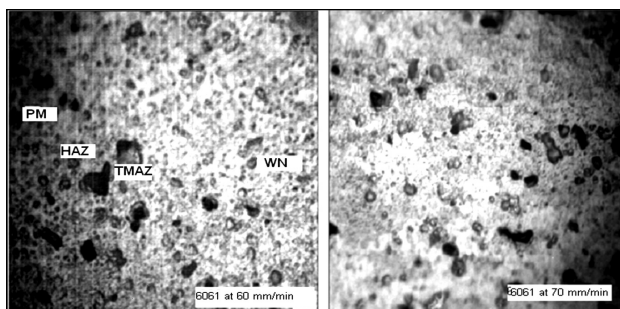
Figure 10: Optical micrograph of AA6061 at 60 mm/min and 70 mm/min
Slika 10: Mikrostruktura spoja AA6061 pri 60 mm/min in 70 mm/min

vided by the rubbing of the tool shoulder and the mechanical stirring of the material by the tool nib, and the adiabatic heat arising from the deformation induced a dynamic recrystallization, showing a transition of aluminium from the parent material to the FSW zone with a clean decrease in the grain size.

3.3 Fractography analysis

An examination of the tensile-fracture surfaces of AA6061 was done at low magnification as well as at higher magnification in order to identify the fracture mechanisms. The SEM observations of the fracture surfaces of the tensile-test specimens revealed the best bonding characteristics of the FSW joints. The fracture surface was found to have very fine dimples revealing a
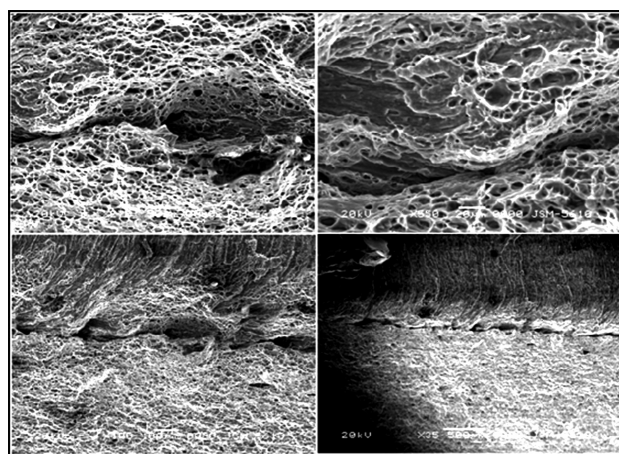
Figure 11: SEM images of the tensile-fracture surface of AA6061 at 65 mm/min
Slika 11: SEM-posnetki preloma pri natezni obremenitvi AA6061 pri 65 mm/min

very ductile behaviour of the material before the failure as shown in **Figure 11**.

3.4 Corrosion behaviour

The potentiostatic polarization curves for the base alloy and FSW samples in 3.5 % NaCl at room temperature are given in **Figures 12** and **13**. It is shown that the corrosion behavior of the parent alloy significantly differs from that of the welded joints.

Table 3: Result analysis of the corrosion test
Tabela 3: Rezultati pri korozijskih preizkusih

Material of the FSW joint	Welding speed (mm/min)	$I_{corr}/(\mu A/cm^2)$	$E_{corr}/$ mV	Corrosion rate (mpy)
$6061T_6$-$6061T_6$	55	471 nA/cm^2	–841	215.3 E^{-3}
$6061T_6$-$6061T_6$	60	202.0 nA/cm^2	–789	92.23 E^{-3}
$6061T_6$-$6061T_6$	65	3.34	–1.35V	1.526
$6061T_6$-$6061T_6$	70	1.35	–1200	617.7 E^{-3}
PM AA6061T$_6$	–	1.820	–1160	832.1 E^{-3}

From **Table 3** it is clear that the pitting potentials of the corrosion-test samples at various process parameters indicate a greater corrosion resistance of the weld metal than of the base metal. This is attributed to the precipitates present in the alloy promoting the matrix dissolution through a selective dissolution of aluminium from the particles. These precipitate deposits are highly cathodic compared to the metallic matrix, initiating the pitting on the surrounding matrix and also enhancing pit growth. During the FSW process only the coarse precipitates could nucleate and grow but not the finer ones. This supported the formation of a passive film, which remained more intact on the surface of the sample. It is also found that in AA6061 and at 65 mm/min, the corrosion resistance is very poor. The poor pitting-corrosion resistance of a weld joint is due to a difference in the pitting potentials across the weld region, or the stir
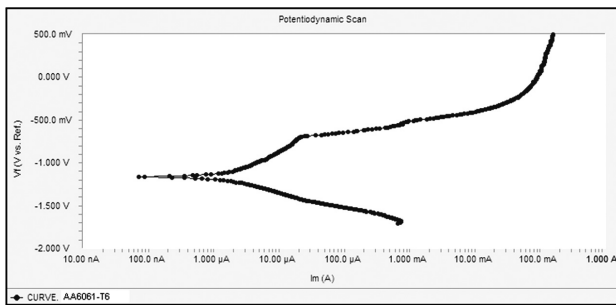
Figure 12: Polarization curves of the AA6061-T$_6$ parent metal
Slika 12: Polarizacijska krivulja osnovne zlitine AA6061-T$_6$
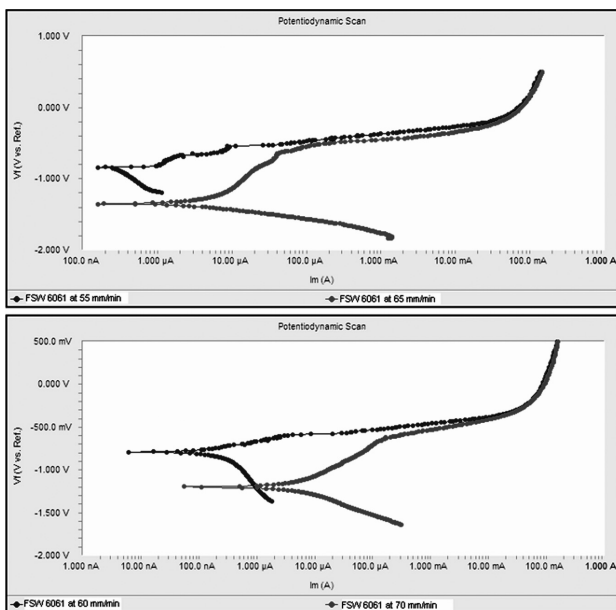
Figure 13: Polarization curves of AA6061 at the welding speeds of 55–70 mm/min
Slika 13: Polarizacijske krivulje AA6061 pri hitrostih varjenja 55–70 mm/min

nugget, caused by the inhomogeneity of the microstructures in these regions. All the FSW samples show a passivation after a longer time of an exposure to the corrosion media. At 65 mm/min, AA6061 has the highest active potential (–1.35 V). The active E_{corr} increased with the increasing weld speed.

4 CONCLUSIONS

The mechanical and metallurgical behavior of AA6061 was studied in this paper. The joints were produced at different welding speeds from 55 mm/min to 70 mm/min and the constant rotational speed of 1700 r/min. The downward force was observed to be constant at 11 kN and it was found to be independent of the weld process parameter for all the produced joints. The tensile strength of a FSW joint is lower than that of the parent metal. With an increase in the welding speed above the critical value, the tensile strength and the fraction of elongation decrease due to a low heat input at the constant downward pressure and the tool rotational speed.

Of the four different welding speeds (55–70 mm/min), the joints fabricated at the welding speed of 55 mm/min exhibited superior tensile properties of 184 N/mm^2 (UTS) and the joint efficiency of 49.32 %. The microstructural changes induced by the FSW process were clearly identified in this study. FSW of AA6060-T$_6$ resulted in dynamically recrystallized zones, TMAZ and HAZ. A softened region has clearly occurred in the friction-stir-welded joints, due to dissolution of the strengthening precipitates. The fracture surface appears to have very fine dimples revealing a very ductile behaviour of the material before the failure. The corrosion rate is increased by increasing the welding speed of the FSW tool.

5 REFERENCES

[1] K. Elangovan, V. Balasubramanian, S. Babu, Predicting tensile strength of friction stir welded AA6061 aluminium alloy joints by a mathematical model, Materials and Design, 30 (**2009**), 188–193

[2] W. M. Thomas et al., Friction stir welding, International Patent Application, No. PCT/GB92/02203 and GB Patent Application No. 9125978.8, December 1991, US Patent No. 5,460,317, 1991

[3] P. L. Threadgill, Friction stir welding – The state of the art, TWI, Bulletin 678, UK, 1999

[4] M. Peel, A. Steuwer, M. Preuss, P. J. Withers, Microstructure, mechanical properties and residual stresses as a function of welding speed in AA5083 friction stir welds, Acta Mater, 51 (**2003**), 4791–801

[5] R. S. Mishra, Z. Y. Ma, Friction stir welding and processing, Materials Science and Engineering: R: Reports, 50 (**2005**), 1–78

[6] N. Li, T. Y. Pan, R. P. Cooper, D. Q. Houston, Z. Feng, M. L. Santella, FSW of magnesium alloy AM60, 19Magnesium Technology 2004, Edited by A. A. Luo, TMS (The Minerals, Metals & Materials Society), 2004

[7] J. Adamowski, M. Szkodo, Friction Stir Welds (FSW) of aluminum alloy AW6082-T6, Journal of Achievement in Materials and Manufacturing Engineering, 20 (**2007**) 1–2, 403–406

[8] R. Palanivel, P. Koshy Mathews, N. Murugan, Influences of tool pin profiles on the mechanical and metallurgical properties of FSW of dissimilar alloys, International Journal of Engineering Science and Technology, 2 (**2010**) 6, 2109–2115

[9] M. Indira Rani, R. N. Marpu, A. C. S. Kumar, A study of process parameters of friction stir welded AA 6061 aluminum alloy in O and T6 conditions, ARPN Journal of Engineering and Applied Sciences, 6 (**2011**) 2, 61–66

[10] L. E. Murr, R. D. Flores, O. V. Flores, J. C. McClure, G. Liu, D. Brown, Friction-stir welding: microstructural characterization, Mater Res Innov., 1 (**1998**) 4, 211–23

[11] H. Liu, H. Fujii, M. Maeda, K. Nogi, Heterogeneity of mechanical properties of friction stir welded joints of 1050-H 24 aluminium alloy, J. Mater. Sci. Lett., 22 (**2003**), 441–4

[12] H. J. Liu, H. Fujii, M. Maeda, K. Nogi, Mechanical properties of friction stir welded joints of 1050-H 24 aluminium alloy, Sci. Technol. Weld Join, 8 (**2003**) 6, 450–4

[13] C. S. Paglia, K. V. Jata, R. G. Buchheit, A cast 7050 friction stir weld with scandium: microstructure, corrosion and environmental assisted cracking, Material Science Engineering- A, 424 (**2006**), 196–204

[14] R. W. Fonda, P. S. Pao, H. N. Jones, C. R. Feng, B. J. Connolly, A. J. Davenport, Microstructure, mechanical properties, and corrosion of friction stir welded Al 5456, Material Science Engineering- A, 519 (**2009**), 1–8

[15] D. A. Wadeson, X. Zhou, G. E. Thompson, P. Skeldon, L. Djapic Oosterkamp, G. Scamans, Corrosion behaviour of friction stir

welded AA7108 T79 aluminium alloy, Corrosion Science, 48 (**2006**), 887–897

[16] M. Jariyaboon, A. J. Davenport, R. Ambat, B. J. Connolly, S. W. Williams, D. A. Price, The effect of welding parameters on the corrosion behaviour of friction stir welded AA2024–T351, Corrosion Science, 49 (**2007**), 877–909

[17] P. S. Pao, S. J. Gill, C. R. Feng, K. K. Sankaran, Corrosion-fatigue crack growth in friction stir welded Al 7075, Scripta Materiala, 45 (**2001**), 605–612

[18] K. Surekha, B. S. Murty, R. K. Prasad, Effect of processing parameters on the corrosion behaviour of friction stir processed AA2219 aluminium alloy, Solid State Sciences, 11 (**2009**), 907–91